Predicting Functional Force Production Capabilities of Upper Extremity Functional Electrical Stimulation Neuroprostheses: A Proof of Concept Study

Eric M. Schearer[1,2,3] **and Derek N. Wolf**[1,2]

[1]Center for Human-Machine Systems, Cleveland State University, Cleveland U.S.A.

[2]Cleveland Functional Electrical Stimulation Center, Cleveland U.S.A.

[3]MetroHealth Medical Center, Department of Physical Medicine and Rehabilitation, Cleveland U.S.A.

Abstract.
Objective. This study's goal was to demonstrate person-specific predictions of the force production capabilities of a paralyzed arm when actuated with a functional electrical stimulation (FES) neuroprosthesis. These predictions allow us to determine, for each hand position in a person's workspace, if FES activated muscles can produce enough force to hold the arm against gravity and other passive forces, the amount of force the arm can potentially exert on external objects, and in which directions FES can move the arm.
Approach. We computed force production predictions for a person with high tetraplegia and an FES neuroprosthesis used to activate muscles in her shoulder and arm. We developed Gaussian process regression models of the force produced at the end of the forearm when stimulating individual muscles at different wrist positions in the person's workspace. For any given wrist position, we predicted all possible forces a person can produce by any combination of individual muscles. Based on the force predictions, we determined if FES could produce force sufficient to overcome passive forces to hold a wrist position, the maximum force FES could produce in all directions, and the set of directions in which FES could move the arm. To estimate the error in our predictions, we then compared our force predictions based on single-muscle models to the actual forces produced when stimulating combinations of the person's muscles.
Main results. Our models classified the person's ability to hold static arm positions correctly for 83% (Session #1) and 69% (Session #2) for 39 wrist positions over two sessions. We predicted this person's ability to produce force at the end of her arm with an RMS error of 5.5 N and the percent of directions for which FES could achieve motion with RMS error of 10%. The accuracy of these predictions is similar to that found in the literature for FES systems with fewer degrees of freedom and fewer muscles.
Significance. These person and device-specific predictions of functional capabilities of the arm allow neuroprosthesis developers to set achievable functional objectives for the systems they develop. These predictions can potentially serve as a screening tool for clinicians to use in planning neuroprosthetic interventions, greatly reducing the risk and uncertainty in such interventions.

1. Introduction

Tetraplegia, which affects roughly 169,000 people in the United States (NSCISC 2018), is a particularly debilitating condition. People with tetraplegia have limited mobility and lack ability to use their arms and hands to complete activities of daily living. Therefore, people with tetraplegia need regular assistance from a caregiver with some people requiring 24-hour assistance.

The main rehabilitation priority for people with tetraplegia is the restoration of arm and hand function (Anderson 2004). Arm and hand function are critical to activities of daily living that allow a person to live independently. These activities include getting dressed, cooking, eating, bathing, and grooming.

Neuroprostheses using functional electrical stimulation (FES) are a promising avenue to restore arm and hand functions. The Freehand System has restored grasping to many people with C5 and C6 spinal cord injuries who have volitional control of their shoulders and elbows (Peckham, Keith, Kilgore, Grill, Wuolle, Thrope, Gorman, Hobby, Mulcahey, Carroll, Hentz & Wiegner 2001). A recent advance uses an implanted brain-computer interface to control hand movements with FES (Bouton, Shaikhouni, Annetta, Bockbrader, Friedenberg, Nielson, Sharma, Sederberg, Glenn, Mysiw et al. 2016). For people with C4 or above injuries, who do not have volitional control of their shoulders or elbows, success of neuroprostheses has been

limited. The Cleveland FES Center has demonstrated preprogrammed shoulder and arm movements with an implanted neuroposthesis (Memberg, Polasek, Hart, Bryden, Kilgore, Nemunaitis, Hoyen, Keith & Kirsch 2014) and more flexible movements commanded by a brain-computer interface with the shoulder actuated by a powered orthosis and the elbow and hand actuated by FES (Ajiboye, Willett, Young, Memberg, Murphy, Miller, Walter, Sweet, Hoyen, Keith et al. 2017). The MUNDUS project demonstrated sequential single joint movements with surface FES and a lockable exoskeleton (Pedrocchi, Ferrante, Ambrosini, Gandolla, Casellato, Schauer, Klauer, Pascual, Vidaurre, Gföhler et al. 2013). The Tools for Brain-Computer Interaction FES+orthosis system demonstrated limited functional movements of the elbow, wrist, and hand (Rohm, Schneiders, Müller, Kreilinger, Kaiser, Müller-Putz & Rupp 2013). These systems are limited in their versatility and robustness and have not restored arm and hand function to people with high tetraplegia for everyday use.

The degree to which function can be restored by a neuroprosthesis for a specific person is uncertain for people with high tetraplegia. This is because the responsiveness of muscles to electrical stimulation is heterogeneous. Lower motor neuron damage causes some muscles to have weak or no response to electrical stimulation (Peckham, Mortimer & Marsolais 1976, Mulcahey, Smith & Betz 1999), making some functional activities impossible without additional support from an orthosis. Further, people with high tetraplegia have varying degrees of muscle atrophy which might further limit function. Finally, because reaching motions involve complex coordination of multiple muscles, it is difficult to predict the combined effects of denervated and atrophied muscles.

This uncertainty along with the risks of a surgical intervention to install a neuroprosthesis greatly limits the progress that can be made in developing neuroprostheses for people with high tetraplegia. Without a reasonable confidence level that recovery of some function will occur, a prospective participant is unlikely to take the risk of having a neuroprosthesis implanted. Even after implantation, uncertainty in outcomes makes the job of designing FES control strategies more difficult. One might question the value of attempting to restore a specific function if it is unclear if that function is even physically achievable given the person's muscles and the neuroprosthesis. In fact, in our early attempts to control arm movements with a 24-channel implanted FES system, we found that many movements of the arm were not possible and that planning arm movements that are possible is not trivial (Schearer, Liao, Perreault, Tresch, Memberg, Kirsch & Lynch 2015). Knowing what functional capabilities a neuroprosthesis is able to restore would greatly reduce the barriers preventing the development of neuroprostheses for high tetraplegia.

Computer simulation is one avenue to predict the effects of individual muscle groups on the ability to complete functional tasks that require coordination of multiple muscles. Researchers have used computer models to identify important muscle groups for standing posture (Kuo & Zajac 1993). More recently our colleagues used a computer simulation to select a group of muscles that, when activated with FES, could produce a wide range of functional reaching movements (Blana, Hincapie, Chadwick & Kirsch 2013). They used this knowledge to plan surgeries for implanting a neuroprosthesis in a person with high tetraplegia. However, computer simulations are not specific enough to predict the effects of denervation and atrophy in specific people with high tetraplegia, which is a heterogeneous population (Mulcahey et al. 1999).

Recent efforts to screen patients with tetraplegia for lower motor neuron damage (Bryden, Hoyen, Keith, Mejia, Kilgore & Nemunaitis 2016) are a step forward but fall

short of making specific predictions of the potential capabilities of neuroprostheses. These screenings identify which muscles are responsive to FES and which muscles are not. The screenings do not predict the workspace that can be achieved with FES, the forces that the arm can apply with FES, or specific functions that might be restored. They also cannot suggest what might be possible with muscle strengthening, a powered orthosis, or some other intervention to supplement FES. In practice, very few people – those with a plurality of muscles responsive to FES – are deemed suitable neuroprosthesis users. If state-specific shortcomings of FES could be identified for individual persons, many more people could be suitable users of neuroprostheses combining FES and some other intervention.

To lower the barriers in development of FES neuroprostheses for high tetraplegia, our goal is to make person-specific predictions of functional capabilities when using a specific neuroprosthesis. These predictions could aid in person-specific selection of muscles a potential neuroprosthesis might activate in order to plan a surgery to implant electrodes. With these predictions we could also design additional assistive devices such as wearable exosuits (Kadivar, Beck, Rovekamp, O'Malley & Joyce 2017) to augment FES. We could efficiently plan tests demonstrating capabilities that are feasible given a specific person and neuroprosthesis, rather than wasting time and resources attempting to demonstrate capabilities that are not physically possible. There have been exciting advances in fitting parameters of EMG-driven musculoskeletal models to person-specific data (Sartori, Reggiani, Farina & Lloyd 2012, Meyer, Patten & Fregly 2017). However, these methods are not useful for people with complete spinal cord injuries as they cannot volitionally activate muscles to produce EMG.

To move toward the goal of person and device-specific predictions of functional capabilities of the arm, this paper presents a proof of concept study. Specifically, we present a method for predicting and graphically displaying the force production capabilities of a paralyzed arm that is actuated by electrical stimulation of multiple muscles. We present the technical details needed to create these graphical displays, which we call capability maps. We demonstrate the capability map concept by making capability maps for a person with high tetraplegia who has an implanted neuroprosthesis that can electrically stimulate multiple muscles to actuate her shoulder and arm. We quantify the accuracy of our predictions of this person's ability to produce forces at the end of her forearm by comparing the predictions to the actual forces produced via stimulation of multiple muscles. We reported a preliminary version of this work in (Schearer & Wolf 2019).

2. Methods

Capability maps display a person's ability to hold static arm configurations, to produce force, and to move when muscles of the shoulder and arm can be activated with electrical stimulation. Capability maps are derived from person-specific models of the arm's response to electrical stimulation of the muscles. Our models are based on measurements of the force at the end of the forearm in response to electrical stimulation of individual muscles. Using these models we can predict the forces that can be produced by stimulating any combination of muscles and, subsequently, we can predict the directions the wrist can move in and if electrical stimulation can produce forces sufficient to hold a static arm configuration against gravity and other passive forces. These capabilities are displayed for different positions of a person's wrist. This

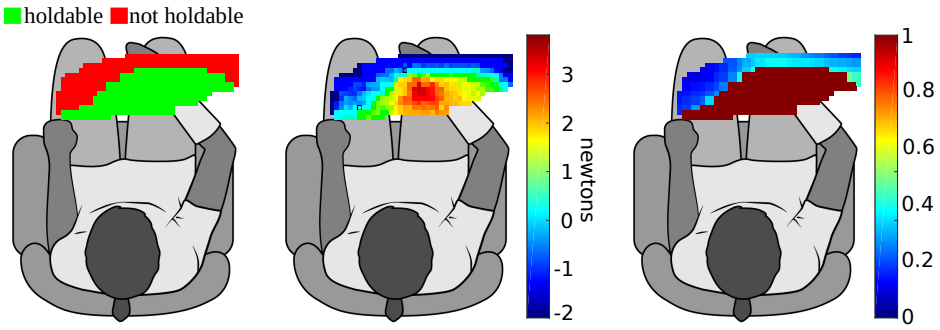

(a) holdability map (b) strength map (c) moveability map

Figure 1. Example of capability maps. The holdability map (a) shows if the person's muscles can produce sufficient force to hold each position given passive forces to overcome. The strength map (b) displays the maximum force magnitude that the person's muscles can produce in all directions with FES. Negative strength indicates that the person cannot produce force in all directions. The moveability map (c) shows the fraction of directions in which the person can produce force at each wrist position. This figure is adapted from (Schearer & Wolf 2019) and is used here with permission.

section describes each of the three types of capability maps, how we gather data to learn the person-specific force production models from which the maps are derived, and how we tested the accuracy of the capability maps in predicting the capabilities of a person with high cervical spinal cord injury and an implanted functional electrical stimulation system.

2.1. Description of capability maps

The most basic capability map is the holdability map (Figure 1(a)). For each wrist position in a person's workspace, the holdability map displays whether or not FES-activated muscles can produce force sufficient to overcome gravity or any other passive forces such as passive muscle stiffness or the stiffness of an orthosis. Note that we use wrist position to refer to the position of the wrist determined by the configuration of the shoulder and elbow joints; we do not mean to describe wrist flexion/extension or abduction/adduction. Holdability for each wrist position is derived from model predictions of the force required to support the arm against passive forces and the forces the muscles can produce to potentially provide this support. A wrist position is holdable if the required passive support force is within the set of forces the muscles can produce when activated with FES. A neuroprosthesis developer or clinician can very quickly look at the holdability map to determine if a neuroprosthesis is likely to provide the ability to hold the wrist at various parts of the workspace. The other two capability maps – the strength map and the moveability map – augment the holdability map with additional information.

The strength map (Figure 1(b)) displays the largest force that the person can apply with FES in all directions for a given wrist position. Strength is displayed for each wrist position with a color scale. The ability to apply a force in a given direction implies that a passive force has already been overcome to then apply this force. For example, if a person cannot lift her/his arm against gravity, she/he cannot produce an upward force when pushing against a fixed object, even though activation of the

deltoids may generally produce an upward force independent of gravity. Strength can be thought of as a graded version of the binary idea of holdability. For a given wrist position, if a person can apply a force in all directions, the wrist position is holdable, and the strength is a positive number. This surplus strength can then be used to push or pull an object in the person's environment. If a person cannot apply a force in all directions, the position is not holdable, and the strength is negative. The magnitude of the negative strength represents the amount of additional force that needs to be provided by an additional assistive device or strengthening of muscles to make a wrist position holdable. A clinician or neuroprosthesis designer can look at the strength map for a spatial representation of the size forces a person can apply or of a person's deficit in force production capability. The strength map does not tell the absolute largest force or the direction in which it can be applied, nor does it tell the direction of negative strength. To answer these questions, the strength map can refer the neuroprosthesis developer to the force polyhedron (detailed in Section 2.2) which displays all the forces that can be applied at a given wrist position.

The moveability map (Figure 1(c)) is a plot of the fraction of directions for which the muscles can produce force for a given wrist position. We call this the moveability map because we assume that applying a static force in a given direction is analogous to producing a movement in that direction. Moveability is shown via a color scale (blue for zero moveability to red for full moveability). Like strength, moveability is a more descriptive version of the binary concept of holdability. 100% moveability means that force can be applied in all all directions and that the wrist position is holdable. For non-holdable positions, moveability helps the clinician or neuroprosthesis developer quickly see for which wrist positions the person's ability to produce force or move in multiple directions is especially limited. Having identified these wrist positions with limited moveability, the clinician and neuroprosthesis developer can look at the force polyhedron (detailed in Section 2.2) to determine exactly which directions of movement are affected and devise a plan to augment the existing FES capability.

2.2. Derivation of capability maps

Capability maps are derived from person-specific models of the arm's response to electrical stimulation. The models predict the force that the arm applies at the end of the forearm in response to electrical stimulation of individual muscles. The overall force production capability, which we display as a polyhedron of achievable forces, is the linear sum of all combinations of the forces produced by the individual muscles. From this "force polyhedron" we derive the holdability, strength, and moveability at each point in the person's workspace.

We mapped the capabilities of a single human participant with high tetraplegia who has an implanted neuroprosthesis that can electrically stimulate her paralyzed muscles to move her right arm. This participant is most appropriate for this proof of concept study for two reasons: 1) she is a current user of assistive technologies to restore reaching movements and is a member of the relevant population that could benefit from capability mapping; 2) her implanted system, which delivers consistent and targeted muscle stimulation, allows for easier implementation of the proof of concept study than does using surface electrodes. Keep in mind, if capability maps were to be used for planning a surgery to implant FES electrodes, stimulation to predict post-surgery functional capabilities would be provided with surface electrodes.

The participant was a 62-year-old woman who sustained a hemisection of the

Table 1. Stimulation electrodes used

Electrode Placement	Muscles Targeted	Approximate Function	Type	Current Amplitude (mA)	Max Pulse Width (μs)
radial nerve	triceps	elbow extension	nerve cuff	2.1	250
axillary nerve	deltoids	arm abduction	nerve cuff	2.1	55
thoracodorsal nerve	latissimus dorsi	arm adduction	nerve cuff	0.8	41
long thoracic nerve	serratus anterior	scapular abduction	nerve cuff	1.4	20
musculocutaneous nerve	biceps brachialis	elbow flexion	nerve cuff	0.8	71
suprascapular nerve	supraspinatus, infraspinatus	shoulder stability, humeral rotation	nerve cuff	1.4	62
rhomboids	rhomboids	scapular adduction	intramuscular	18.0	155
lower pectoralis	lower pectoralis	shoulder horizontal flexion	intramuscular	18.0	98
upper pectoralis	upper pectoralis	shoulder horizontal flexion	intramuscular	20.0	50

spinal cord at the C1-C2 level from a gunshot wound in 1994. She is unable to move her right arm but does have sensation. She experiences hypertonia in some of the arm muscles. Additionally, the participant's wheelchair is equipped with a passive arm support to assist against the force of gravity. More details can be found in (Polasek, Hoyen, Keith, Kirsch & Tyler 2009) (participant 1). While we can derive capability maps for people with or without the arm support, the current reality for people with high tetraplegia is that holdability, as defined in this paper, is always zero without the arm support. Hence we derive capability maps for the arm including the arm support. The arm support produces a more functional workspace by reducing the passive force the muscles must overcome to hold the arm in a static position.

The participant was implanted with a stimulator-telemeter (Smith, Peckham, Keith & Roscoe 1987, Smith, Tang, Johnson, Pourmehdi, Gazdik, Buckett & Peckham 1998, Hart, Bhadra, Montague, Kilgore & Peckham 2011) in her abdomen in 2005. This device has leads which carry current to intramuscular electrodes (Memberg, Peckham & Keith 1994) and nerve cuff electrodes (Naples & Mortimer 1988) to activate muscles in her right arm and shoulder complex. We refer to each muscle or group of muscles stimulated by a single electrode as a muscle group. In this experiment, we controlled the nine muscle groups shown in Table 1. Power and control signals are sent to the implanted device via an inductive radio-frequency link. Stimulation uses bi-phasic, charge balanced pulses delivered at 13 Hz. The amplitude of the pulses for each muscle group was chosen to produce as large a force response as possible while not causing the participant to feel pain. The force generated by each muscle group is controlled by varying the pulse-width (referred to as the stimulation input) from 0-250 μs. We send stimulation commands to the implant using real-time control code on a computer. Appropriate stimulation and amplitude limits were determined and periodically adjusted for participant safety. A representative set of these limits is shown in Table 1. The controller commands cannot exceed these limits.

(a) (b) (c)

Figure 2. Instrumentation for experiments. Pictured is the participant's right arm. Shown in (a) and (b) are the placement of the rigid bodies with reflective markers for optical tracking, a passive arm support with rubber bands providing supporting force, and the robot that drives the participant's wrist to 27 positions in the participant's workspace. The participant's wrist and distal forearm (c) are in a soft cast that is attached via a magnet to a ball-and-socket joint at the end effector of the HapticMaster robot. This figure was previously published in (Schearer & Wolf 2019) and is used here with permission.

Informed consent was obtained from the research participant and all protocols used for this research were approved by the institutional review boards at Cleveland State University (IRB NO. 30213-SCH-HS) and MetroHealth Medical Center (IRB NO. 04-00014).

Data from which to learn models of the response of the participant's arm to electrical stimulation of individual muscles were collected by gathering force and position data as the person's wrist was moved to and held in various static positions by a HapticMaster (Moog FCS) robot while individual muscles were stimulated (Figure 2). The models and identification procedure are described fully in (Schearer, Liao, Perreault, Tresch, Memberg, Kirsch & Lynch 2016, Wolf & Schearer 2018). The robot has three degrees of movement freedom and records the 3D forces and position of its end effector. The force sensor reports the force required to hold the wrist at a given position, and an Optotrak Certus Motion Capture System (Northern Digital, Inc.) determines the position of the participant's wrist relative to her thorax. The input to the models is the wrist position in Cartesian space measured relative to the participant's thorax. The models' output is the 3D force applied by the robot to hold the wrist position.

At the start of each of two experimental sessions we collected force and position data at 27 different positions of the participant's wrist. The 27 positions were selected by manually moving the participant's wrist in three roughly circular shapes on three horizontal planes. One circle was approximately mouth height, one approximately at the top of the sternum, and one approximately at the bottom of the sternum. Each circle included a center point and eight points distributed approximately evenly around the circumference. We chose this manual strategy for selecting positions because it allowed the participant to define the limits of comfortable arm positions. We would attempt to move her wrist in a given direction until she became uncomfortable, generally due to stiffness. We would then move the wrist back a bit to ensure each position was comfortable for her. At each of the 27 wrist positions we stimulated each of the nine muscle groups shown in Table 1 individually, recording the steady-state force exerted by the robot to hold the position along with the wrist position relative to the thorax. We also recorded the force and wrist position when no muscle groups were

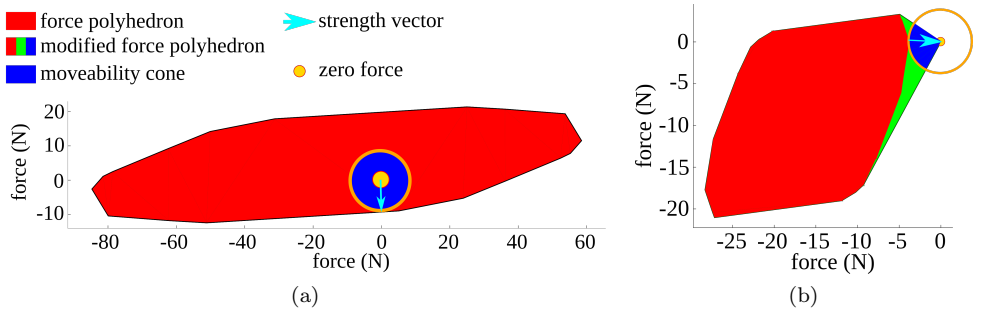

Figure 3. 2D representations of example force polyhedra for a holdable wrist position (a) and a non-holdable position (b). For the holdable position in (a) the origin (gold circle) is inside the force polyhedron (red area) so a force can be applied in any direction, and hence the moveability cone is the entire blue circle. The strength vector (cyan arrow) runs from the origin to the nearest point on the edge of the force polyhedron. The magnitude of the strength vector is the strength – the maximum force that can be applied in any direction. For the non-holdable position in (b) the origin is not inside the force polyhedron. The participant can only apply forces in some directions, namely those in the direction of the force polyhedron. The moveability cone (blue) represents these directions. The moveability cone is the intersection of the modified force polyhedron (red, green, and blue) and a sphere around the origin. The cyan strength vector, which runs from the closest point to the origin on the force polyhedron to the origin, represents the additional force that would need to be produced to make the wrist position holdable.

stimulated. We randomized the order of muscle groups stimulated and wrist positions visited.

With the force and wrist position data we used Gaussian process regression (Rasmussen & Williams 2006) to predict forces at the wrist as a function of wrist position for each muscle group. Gaussian process regression predicts both the force at the wrist required to hold a position when no muscles are stimulated and the forces required to hold a position when a specific muscle group is stimulated. The difference between these two predictions is the amount of force a given muscle group can contribute at each wrist position.

These Gaussian process regression model predictions allow us to construct a 3D polyhedron of forces – the force polyhedron – that the arm can exert with combinations of muscles at any specific wrist position measured relative to the thorax. This is a person-specific implementation of the theoretical force polyhedron introduced in (Valero-Cuevas 2009). To construct the force polyhedron we first compute the Minkowski sum of the vectors of muscle force contributions and then subtract the force required to hold the wrist position against gravity or other position dependent passive forces. For the given wrist position, the resulting force polyhedron represents the convex set of forces that the arm can apply to the robot or any other fixed object. We call this computation of the force polyhedron based on our Gaussian process regression models the "predicted force polyhedron".

We use the predicted force polyhedron to derive the holdability, strength, and moveability at each wrist position. Examples of force polyhedra are shown in Figure 3. A wrist position is holdable (holdability = 1) if the force polyhedron includes the origin as in Figure 3(a). This means that stimulating the muscles can produce the force required to hold the wrist position. If the force polyhedron does not include

the origin, as in Figure 3(b), the wrist position is not holdable (holdability = 0). We define strength as the distance from the origin to the nearest point on the force polyhedron (cyan arrows in Figure 3). When the wrist position is holdable, strength is the maximum force that can be applied in every direction. If a wrist position is not holdable, strength is assigned a negative value and is the minimum additional force required to make the position holdable.

Moveability represents the freedom with which the person's wrist can move for a given wrist position. If stimulating the muscles can produce a force in any direction, moveability equals one as in Figure 3(a). For the most part a holdable wrist position has a moveability of one. The exception is when the force polyhedron has the origin as a boundary, in which case the position is holdable, but moveability is less than one. When moveability is less than one we determine moveability by solving a computational geometry problem using the Multi-Parametric Toolbox 3 (Herceg, Kvasnica, Jones & Morari 2013) for MATLAB; we determine the ratio of the volume of a convex cone – the moveability cone – representing all the directions in 3D that the hand can move, to the volume of a sphere which represents all possible directions. The moveability cone (see Figure 3(b)) is the intersection of a modified force polyhedron – the force polyhedron with the origin as an additional vertex – and a sphere centered at the origin with radius equal to the distance from the origin to the closest neighboring vertex on the modified force polyhedron.

Capability maps display holdability, strength, and moveability at discrete points in the workspace of the participant's wrist. We created a 3-dimensional grid inside the convex hull of all wrist positions visited when gathering data to construct models. At each wrist position we derive the predicted force polyhedron by taking the Minkowski sum of force vectors that our Gaussian process regression models predict for individual muscles. The entire process of setting up experimental equipment, gathering data, and computing and displaying the capability maps takes 45-60 minutes.

2.3. Accuracy of capability maps

To quantify the accuracy of the predicted force polyhedra, we stimulated multiple muscles together to experimentally create the force polyhedra at wrist positions in a 3D grid in the participant's workspace. We define an "experimental force polyhedron" as the convex hull of all the forces achieved when stimulating combinations of muscles that produce the forces at the edges of the predicted force polyhedron – that is, the maximum forces in each direction. Comparing the experimental force polyhedron to the predicted force polyhedron serves to quantify the error in 1) using Gaussian process regression to predict muscle forces at different wrist positions and 2) the assumption that the forces produced when stimulating multiple muscles is the sum of the forces produced when stimulating muscles individually.

From these experimental force polyhedra we computed the holdability, strength, and moveability and compared these values to the holdability, strength, and moveability derived from the predicted force polyhedra. We ran trials simultaneously stimulating multiple muscles to create the experimental force polyhedra during experimental sessions on two separate days in order to compare to predicted force polyhedra derived from single-muscle data collected at the start of each session. In random order we visited evenly spaced wrist positions inside the convex hull of the participant's passive range of motion. 23 wrist positions were visited during the first session and 16 during the second. The number of positions visited each day varied based on the size of the

person's passive range of motion on each day and on the time available to visit wrist positions.

To create the experimental force polyhedron at each wrist position, we stimulated the muscles to apply force to the robot to achieve force targets in multiple directions. For each wrist position we chose the desired force targets from a subset of the vertices of the predicted force polyhedron. Choosing only a subset of vertices for each wrist position allowed us to test more wrist positions than if testing all vertices in each predicted force polyhedron. We refer to the polyhedron bounded by the subset of vertices as the "target force polyhedron". Before the experiment, we increased the size of this subset until the holdability, strength, and moveability of the polyhedron – the target polyhedron – made up of the subset of vertices of the predicted force polyhedron closely matched the holdability, strength, and moveability of the predicted force polyhedron. We required that the holdability be matched exactly, that the strength of the target polyhedron be within 0.5 N of the strength predicted by the predicted force polyhedron, and that the moveability of the target polyhedron be within 0.05 (5 percentage points) of the moveability predicted by the predicted force polyhedron. For a given number of n force targets, we used k-means clustering to create n clusters of vertices of the predicted force polyhedron. For each cluster of vertices, we included the vertex with the largest magnitude as a target force for our experiments. We increased the number n of desired targets until the holdability, strength, and moveability of the target and predicted force polyhedra matched as described above. Depending on this random selection of vertices, the target force polyhedra contained from 5 to 18 vertices.

For each trial we applied open-loop muscle stimulation inputs to attempt to produce the force at each vertex of the target force polyhedron. By definition of the force polyhedron, these stimulation inputs were combinations of either zero or full activation for each muscle group. For each vertex, the stimulation pattern was applied for two seconds followed by two seconds of rest before the stimulation for the next vertex was applied. The average force over the last one half second of stimulation was recorded as the experimental force.

Based on our experiments when stimulating multiple muscles we computed the accuracy of the three capability measures at each wrist position tested. Holdability accuracy is the percent of wrist positions for which the predicted force polyhedron correctly classified the experimentally determined holdability when stimulating multiple muscles. We used a chi-squared test to test the null hypothesis that holdability accuracy is independent across sessions. We used McNemar's test with continuity correction to test the null hypothesis that the matched pairs of holdability values – predicted and experimentally observed – are dependent on each other. If they are dependent, this shows that our predictions match the experimental results. The accuracy of the strength prediction is the difference between the strength of the predicted force polyhedron at each wrist position and the experimentally measured strength. We used a one-way ANOVA to test the null hypothesis that the mean strength prediction error is the same across the two sessions and a one-sample t-test to test the null hypothesis that the mean strength prediction error is zero. Similar calculations were made for moveability. In examining the accuracy of moveability predictions we only included trials for correctly identified non-holdable positions. This is because moveability typically makes an abrupt jump from approximately 40% to 100% as holdability changes from 0 to 1. Including this jump fundamentally changes the moveability from a continuous variable to a hybrid continuous/discrete variable. Further, correct predictions

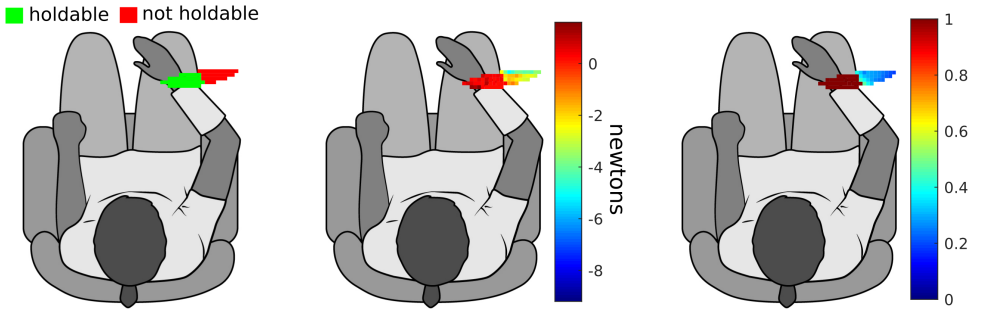

(a) holdability map (b) strength map (c) moveability map

Figure 4. Predicted capability maps computed by Gaussian process regression based on single muscle stimulation data. Pictured are 2D horizontal cross-sections approximately 10 cm below the top of the participant's sternum. Note that other horizontal cross sections can have significantly different holdability, strength, and moveability values.

of 100% moveability for holdable positions are trivial, so including them artificially raises the accuracy of moveability predictions. Statistical analyses were performed using MATLAB (Mathworks, Inc., Natick, MA).

3. RESULTS

3.1. Display of Capability Maps

In this section we give examples of the three types of capability maps: the holdability map, the strength map, and the moveability map (Figure 4). We quantify the accuracy of our models by comparing the models' predictions of holdability, strength, and moveability to the same values determined by stimulating multiple muscles to produce experimental force polyhedra at points of a person's workspace during two experimental sessions. These analyses were carried out for a person with a high cervical spinal cord injury who uses a functional electrical stimulation neuroprosthesis to move her paralyzed arm.

Figure 4 shows the predicted capability maps as calculated by our Gaussian process regression models based on single muscle data. We should note that the participant in this study has a rather limited passive range of motion as represented by the colored areas in Figure 4. The capability maps display this person's force production capabilities within the passive range of motion. Her limited passive range of motion is due mainly to increased tone in her shoulder and pectorals making larger movements across her body or out to the right side of her body painful for her. The limited range of motion does not, however, affect her ability to produce force within the passive range of motion, which we capture with capability maps.

The predicted holdability map (Figure 4(a)) displays green if the participant's muscles can produce enough force to hold the wrist position against the passive stiffness of her arm and the arm support. Otherwise it displays red. The holdable wrist positions (green) for this person are on the left side of the participant's passive range of motion. The non-holdable positions are on the right side where holding a position requires more shoulder horizontal abduction.

Table 2. Accuracy of Capability Maps.

	holdability	strength error (N)			moveability error		
	(% correct)	mean	mean$\neq 0$	RMS	mean	mean$\neq 0$	RMS
Session #1	83	3.0		6.0	0.0006		0.10
Session #2	69	0.5		4.6	-0.02		0.10
Overall	77	2.0	yes, $p = 0.02$	5.5	-0.09	no, $p = 0.65$	0.10
Session effect?	yes		no			no	

The predicted strength map (Figure 4(b)) displays the largest force that the person can apply in all directions. Positive strength means that the person can apply force in all directions at the given wrist position (red area of Figure 4(b)). There are also wrist positions at which the person cannot produce force in all directions (orange, yellow, and green areas of Figure 4(b)). For these wrist positions the strength is a negative number representing the magnitude of additional force the muscles would need to produce to make that wrist position holdable. The highest strength for this person was 1.3 N at a wrist position near the person's sagittal plane. This is roughly enough strength to hold and move a fork or push a button but not enough to move heavier objects. The lowest strength was -16.8 N at a position high and to the right, which is not pictured in the 2D cross section in Figure 4(a). At high wrist positions, the person could not exert upward forces.

The predicted moveability map (Figure 4(c)) displays the percentage of 3D directions for which the participant's muscles can produce force and hence motion. The participant can produce force in all directions (dark red in Figure 4(c)) for holdable wrist positions (green in Figure 4(b)). At non-holdable positions moveability is less than 100% – around 40% near the boundary of the holdable region (light blue in Figure 4(c)) and decreasing for wrist positions further to the right of the holdable region (dark blue in Figure 4(c)). At these non-holdable positions, the participant can produce forces toward the holdable positions but not in other directions.

Note that the individual capability maps are interrelated. Wrist positions that are holdable have positive strength and 100% moveability. Wrist positions that are not holdable have negative strength and moveability less than 100%. The strength map continuously quantifies force production capability at holdable positions and force production deficits at non-holdable positions. The moveability map continuously quantifies capabilities at non-holdable positions.

3.2. Accuracy of Capability Maps

To quantify the accuracy of the capability maps, we produced experimental force polyhedra at various wrist locations in the person's workspace during each of two experiment sessions. At each wrist location we computed the holdability, strength, and moveability of the force polyhedron and compared them to the same measures for the target force polyhedron. Recall that the target force polyhedron, made of a subset of vertices of the predicted force polyhedron, closely matches the holdability, strength, and moveability of the predicted force polyhedron. A summary of these results is included in Table 2.

Our models correctly predicted holdability for 19 of 23 (83%) wrist positions visited during Session #1 and 11 of 16 (69%) positions during Session #2. We fail to

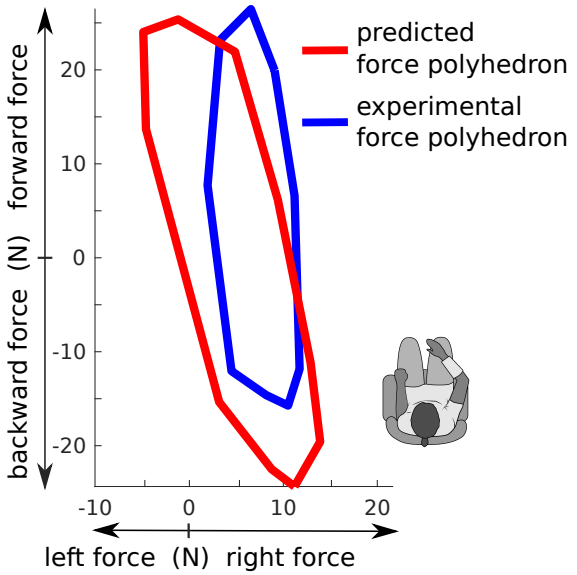

Figure 5. Predicted and experimental force polyhedra for a wrist position that is 2 cm to the right of the participant's sternum, 3 cm below the top of the sternum, and 35 cm in front of the sternum. Data to build a model to predict force production capability and data collected to experimentally validate the force polyhedron was collected during Session #2. The picture of the person on the lower right part of the figure is to orient the reader to the directions of forces displayed in the force polyhedra. The polyhedra are 2D representations of 3D force polyhedra.

reject the null hypothesis that the holdability accuracy of the two sessions are independent ($p = 0.31$). This dependence on session is reasonable as making correct holdability predictions depends on the frequency of positions being near the borderline of holdability, which depends on the placement of the person's arm in her arm support and her day-to-day level of muscle tone and strength. There was no significant difference between the target and experimental holdability for either of the two sessions ($p = 0.62$ for Session #1 and $p = 1$ for Session #2).

Over two sessions the average error in predicting strength was 2.0 N, and the mean error was significantly different than zero ($p = 0.02$). This indicates that the strength measured in experiments when stimulating multiple muscles was typically larger than the strength calculated based on our muscle models. The root mean squared error in strength predictions was 5.5 N. For comparison, the smallest strength value over both sessions for this participant was -20.6 N, and the largest strength value was 1.2 N. There was no significant effect of session on the error in strength ($p = 0.13$).

For non-trivial cases – those with moveability less than one – our model's average error in predicting moveability was -0.009, or less than one percentage point in absolute value, reported as a fraction of directions in which the muscles can produce force. The mean error was not significantly different than zero ($p = 0.65$) which means that there was no bias toward either overestimating or underestimating moveability. The root mean squared error was 0.10. For non-trivial cases, the moveability range was 0.02 to 0.39. The session had no significant effect on moveability error ($p = 0.57$).

To illustrate the numerical results we report above, Figure 5 shows the experimen-

tal and target force polyhedra for a trial with holdability, strength, and moveability close to the root mean squared error for each value. In this "average" case, the experimental force polyhedron correctly classifies the wrist/arm position as not holdable, has an error in predicting strength of -4.7 N (0.2 N less in magnitude than the RMS strength error), and an error in predicting moveability of -0.2 (0.1 more in magnitude than the RMS moveability error). The error in prediction of strength for the force polyhedra in Figure 5 is larger than the errors for 16 other wrist positions and smaller than 22 other positions. For non-trivial cases the moveability prediction error for the force polyhedra in Figure 5 is larger than the errors for 25 other wrist positions and smaller than 1 other positions. The experimental force polyhedron has similar magnitude, shape, and orientation as the predicted force polyhedron. Both polyhedra indicate that the person can produce larger forward/backward forces than right/left forces largely due to the triceps, which produces primarily a forward force in this wrist position, and biceps, which produces primarily a backward force, being the muscles that produce the largest forces for this person. The experimental force polyhedron is slightly rotated clockwise relative to the predicted force polyhedron. The experimental polyhedron also shows less force production capability in the backward direction than the predicted polyhedron.

4. Discussion

This paper presents the concept of the capability map which has the potential to lower barriers to development and use of neuroprosthetic devices to restore movement to people with paralyzed arms. This proof of concept study describes the derivation of capability maps, demonstrates their use for a person with high tetraplegia with an implanted FES neuroprosthesis, and quantifies their accuracy. By predicting the forces required to hold static wrist positions and the forces that a person's muscles can produce, we can predict a person's capability to hold static wrist positions (holdability), produce forces at the end of the forearm (strength), and move in certain directions (moveability). This process allows us to predict person and device-specific force production capabilities.

The strength predictions of our capability maps showed similar accuracy to various FES force and torque controllers reported in the literature. We use the force/torque control comparison because capability maps are based on predictions of muscle force evoked by FES. The 5.5 N RMS error in our strength predictions is 12% of the maximum force of 44.9 N that the participant could produce during experiments. Open loop force control with the same participant yielded 11% errors (Schearer, Liao, Perreault, Tresch, Memberg, Kirsch & Lynch 2014b) and torque predictions in dynamic movements had errors under 20% (Schearer et al. 2016). In testing similar models of FES force production, one group reported RMS isometric force errors of 2.3 N to 5.7 N for 5 N magnitude force targets across three healthy subjects (Razavian, Ghannadi, Mehrabi, Charlet & McPhee 2018). A closed-loop FES controller achieved ankle torque accuracy ranging from 4% to 11% of torque capacity for able-bodied participants (Zhang, Hayashibe & Azevedo-Coste 2013). Isometric knee torques were controlled with closed-loop electrical stimulation of the quadriceps with 1.45 Nm RMS error across eight healthy participants (Merad, Downey, Obuz & Dixon 2015); this is error is approximately 6% of the approximately 23 Nm maximum torque reported. Our predictions should be considered the equivalent of an open-loop

controller without the benefit of feedback. Also consider that we used nine muscles that actuate the shoulder and elbow to control forces. The smaller errors reported in (Zhang et al. 2013) and (Merad et al. 2015) use feedback to control one joint with one muscle for participants without neurological impairments.

The most immediate use of capability maps is in developing FES controllers of reaching movements. We developed capability maps in response to discovering in early motion control trials that many movements at various speeds were impossible according to our local models of FES force production (Schearer et al. 2015). With capability maps we can more intelligently plan movements that can be achieved by avoiding non-holdable wrist positions and avoiding planning movements in non-moveable directions. Capability maps also allow us to increase the number of holdable positions by making adjustments to the stiffness of the mobile arm support or position of the participant's arm in the arm support.

With further refinement we envision capability maps as a means of predicting functional outcome measures and as a tool for recommending interventions to improve functional outcomes. Capability maps offer a level of detail at the joint and muscle level that can enhance understanding of a person's limitations and potential solutions to increase capability rather than merely evaluating capability broadly. Consider for instance a clinical measure such as the Capabilities of Upper Extremity Instrument Push/Pull Test (Marino, Shea & Stineman 1998). In this test a person attempts to push and pull a pot from one place on a table to another with increasing weights in the pot. The test does not give insight into what must be done to increase the score. Capability maps could pinpoint weakness in a specific muscle or inability to apply force in a specific direction. These shortcomings might be addressed with muscle strengthening, tendon transfers, or the design of a powered orthosis depending on the specific case. We note that this proof of concept study used implanted electrodes, while eventual use of capability maps will use surface electrodes to inform intervention strategies. Predictions with surface electrodes may have more uncertainty than the results reported in this paper.

Capability maps will require more user-friendly and faster data collection to make them useful as a clinical tool. The current system to construct capability maps lasts 45-60 minutes and requires expensive equipment and expert support. We gathered data to construct capability maps using a laboratory motion capture system and a robot, which require significant setup time and technical support. Many researchers have used low-cost commercial video game motion tracking systems successfully for similar purposes (Han, Shao, Xu & Shotton 2013). The robot used in gathering data to create the capability maps acts as a mobile force sensor. It could be replaced by a sensor worn on the participant's wrist while a therapist moves the participant's wrist by applying force at the sensor (Hetrick, Guillen & Schearer 2017).

Further, capability maps will need more automated interpretation for clinical use. The maps we show in this paper are useful simplifications of a person's force production capabilities, but they do not tell the whole story. They very quickly allow a clinician to see for which parts of a person's workspace capabilities are limited. To make a meaningful change to an intervention strategy, a clinician would have to refer to a more detailed representation of capability, such as the force polyhedra presented in this paper. We envision a semi-automated multi-level system where a clinical team views the capability maps and touches a screen in an area of interest on the map to open up a picture of the force polyhedron for that area. Clinicians could then have the option of experimenting with enhancements of muscle strength or addition

of capabilities via an orthosis that would change the force polyhedra and capability maps. This would allow them to assess how these enhancements might affect function. The clinical team could interact with these layers of detail to plan interventions. We see improved automation as a technical challenge that will be overcome in time rather than as a fundamental impediment to clinical use of capability maps.

A limitation of capability maps as they are presented here is that they are only for static wrist positions. We can very easily extend the idea to dynamic movements where our capability maps become functions of both position and velocity. This extension will allow us to predict the arm's ability to perform a specific task at a desired speed and identify muscles that need to be strengthened or degrees of freedom for which torque requirements are high. We have already created such dynamic models (Schearer et al. 2016) and used them to determine if given wrist trajectories are possible (Schearer et al. 2015).

Although we demonstrated the concept of capability maps for a person with high tetraplegia, the idea can be extended to other upper extremity impairments. High tetraplegia was an obvious place to start as this person has essentially no capability for volitional movements. We did not have to distinguish between the effects of FES or any other assistive technology and the effects of volitional movements. For people with various arm impairments and capabilities resulting from stroke, multiple-sclerosis, traumatic brain injury, muscular dystrophy and other neuromuscular conditions the problem of creating our force-based models becomes more challenging. We see this challenge as an issue of experiment design to learn models of the arm for people with volitional control rather than a fundamental roadblock to mapping the capabilities of people with arm impairments besides high tetraplegia. We have designed experiments to create holdability maps for healthy participants (Schearer, Liao, Perreault, Tresch, Memberg, Kirsch & Lynch 2014a) and all three capability maps for a person with high tetraplegia. Now the challenge becomes mapping capabilities along the entire spectrum of volitional control of the arm. For people with conditions other than complete paralysis, we can still stimulate muscles with FES and measure the output of individual muscles at different wrist positions – we just need to design the experiment to separate the effects of stimulation of a single muscle from effects caused by a participant inadvertently activating other muscles at the same time.

We should be careful to state that the knowledge of muscle strength displayed by capability maps does not link directly to function for people with conditions other than complete paralysis. The link between strength and function has been documented for multiple sclerosis (Dalgas, Stenager & Ingemann-Hansen 2008, Dalgas, Stenager, Jakobsen, Petersen, Hansen, Knudsen, Overgaard & Ingemann-Hansen 2009), muscular dystrophy (McDonald, Abresch, Carter, Fowler Jr, Johnson, Kilmer & Sigford 1995), stroke (Bohannon 2007), traumatic brain injury (Duong, Englander, Wright, Cifu, Greenwald & Brown 2004), and incomplete spinal cord injury (Kim, Eng & Whittaker 2004). However, we see the ability to map muscle strength in a person's workspace as a vital tool to increasing understanding of how muscle strength and function are related.

This initial proof of concept of capability maps shows their potential to be an important tool for upper extremity rehabilitation research and practice. The idea of examining the effects of specific muscle groups on capability is not new, as researchers have used computer models to identify important muscle groups for standing posture (Kuo & Zajac 1993) and more recently for arm movements (Blana et al. 2013). The innovation in the work presented in this paper is that we can map the capabilities of

specific people rather than of computer models. By creating person-specific models of the arm's capabilities we can give researchers and clinicians straight-forward insights into why a specific person using a specific device lacks an upper extremity capability and how that capability might be improved with an appropriate intervention.

5. Acknowledgements

We thank Debbie Espy, PT, PhD and Ann Reinthal, PT, PhD, NCS for their ideas on the applicability of capability maps to a broader range of neuromuscular disorders. We also thank Ron Hart and Bill Memberg for their help with addressing technical challenges in experimental sessions.

References

Ajiboye, A. B., Willett, F. R., Young, D. R., Memberg, W. D., Murphy, B. A., Miller, J. P., Walter, B. L., Sweet, J. A., Hoyen, H. A., Keith, M. W. et al. (2017). Restoration of reaching and grasping movements through brain-controlled muscle stimulation in a person with tetraplegia: a proof-of-concept demonstration, *The Lancet* **389**(10081): 1821–1830.

Anderson, K. D. (2004). Targeting recovery: Priorities of the spinal cord-injured population, *Jounral of Neurotrauma* **21**(10): 1371–1383.

Blana, D., Hincapie, J. G., Chadwick, E. K. & Kirsch, R. F. (2013). Selection of muscle and nerve-cuff electrodes for neuroprostheses using customizable musculoskeletal model, *Journal of Rehabilitation Research & Development* **50**(3): 395–408.

Bohannon, R. W. (2007). Muscle strength and muscle training after stroke, *Journal of rehabilitation Medicine* **39**(1): 14–20.

Bouton, C. E., Shaikhouni, A., Annetta, N. V., Bockbrader, M. A., Friedenberg, D. A., Nielson, D. M., Sharma, G., Sederberg, P. B., Glenn, B. C., Mysiw, W. J. et al. (2016). Restoring cortical control of functional movement in a human with quadriplegia, *Nature* **533**(7602): 247.

Bryden, A. M., Hoyen, H. A., Keith, M. W., Mejia, M., Kilgore, K. L. & Nemunaitis, G. A. (2016). Upper extremity assessment in tetraplegia: the importance of differentiating between upper and lower motor neuron paralysis, *Archives of physical medicine and rehabilitation* **97**(6): S97–S104.

Dalgas, U., Stenager, E. & Ingemann-Hansen, T. (2008). Multiple sclerosis and physical exercise: recommendations for the application of resistance, endurance, and combined training, *Multiple Sclerosis Journal* **14**(1): 35–53.

Dalgas, U., Stenager, E., Jakobsen, J., Petersen, T., Hansen, H. J., Knudsen, C., Overgaard, K. & Ingemann-Hansen, T. (2009). Resistance training improves muscle strength and functional capacity in multiple sclerosis, *Neurology* **73**(18): 1478–1484.

Duong, T. T., Englander, J., Wright, J., Cifu, D. X., Greenwald, B. D. & Brown, A. W. (2004). Relationship between strength, balance, and swallowing deficits and outcome after traumatic brain injury: A multicenter analysis, *Archives of physical medicine and rehabilitation* **85**(8): 1291–1297.

Han, J., Shao, L., Xu, D. & Shotton, J. (2013). Enhanced computer vision with microsoft kinect sensor: A review, *IEEE transactions on cybernetics* **43**(5): 1318–1334.

Hart, R. L., Bhadra, N., Montague, F. W., Kilgore, K. L. & Peckham, P. H. (2011). Design and testing of an advanced implantable neuroprosthesis with myoelectric control, *IEEE Transactions on Neural Systems and Rehabilitation Engineering* **19**(1): 45–53.

Herceg, M., Kvasnica, M., Jones, C. & Morari, M. (2013). Multi-Parametric Toolbox 3.0, *Proc. of the European Control Conference*, Zürich, Switzerland, pp. 502–510. http://control.ee.ethz.ch/ mpt.

Hetrick, B., Guillen, C. & Schearer, E. (2017). Wearable force/torque sensor for updating models of paralyzed arms, *Proceedings of the International Symposium on Wearable and Rehabilitaton Robotics*, IEEE.

Kadivar, Z., Beck, C. E., Rovekamp, R. N., O'Malley, M. K. & Joyce, C. A. (2017). On the efficacy of isolating shoulder and elbow movements with a soft, portable, and wearable robotic device, *Wearable Robotics: Challenges and Trends*, Springer, pp. 89–93.

Kim, C. M., Eng, J. J. & Whittaker, M. W. (2004). Level walking and ambulatory capacity in

persons with incomplete spinal cord injury: relationship with muscle strength, *Spinal Cord* **42**(3): 156.

Kuo, A. D. & Zajac, F. E. (1993). A biomechanical analysis of muscle strength as a limiting factor in standing posture, *Journal of Biomechanics* **26**: 137–150.

Marino, R. J., Shea, J. A. & Stineman, M. G. (1998). The capabilities of upper extremity instrument: reliability and validity of a measure of functional limitation in tetraplegia, *Archives of physical medicine and rehabilitation* **79**(12): 1512–1521.

McDonald, C. M., Abresch, R. T., Carter, G. T., Fowler Jr, W. M., Johnson, E. R., Kilmer, D. D. & Sigford, B. J. (1995). Profiles of neuromuscular diseases: Duchenne muscular dystrophy., *American journal of physical medicine & rehabilitation* **74**(5): S93.

Memberg, W. D., Peckham, P. H. & Keith, M. W. (1994). A surgically-implanted intramuscular electrode for and implantable neuromuscular stimulation system, *IEEE Transactions on Rehabilitation Engineering* **2**(2): 80–91.

Memberg, W. D., Polasek, K. H., Hart, R. L., Bryden, A. M., Kilgore, K. L., Nemunaitis, G. A., Hoyen, H. A., Keith, M. W. & Kirsch, R. F. (2014). Implanted neuroprosthesis for restoring arm and hand function in people with high level tetraplegia, *Archives of Physical Medicine and Rehabilitation* **95**(6): 1201–1211.

Merad, M., Downey, R. J., Obuz, S. & Dixon, W. E. (2015). Isometric torque control for neuromuscular electrical stimulation with time-varying input delay, *IEEE Transactions on Control Systems Technology* **24**(3): 971–978.

Meyer, A. J., Patten, C. & Fregly, B. J. (2017). Lower extremity emg-driven modeling of walking with automated adjustment of musculoskeletal geometry, *PloS one* **12**(7): e0179698.

Mulcahey, M., Smith, B. & Betz, R. (1999). Evaluation of the lower motor neuron integrity of upper extremity muscles in high level spinal cord injury, *Spinal Cord* **37**(8): 585.

Naples, G. G. & Mortimer, J. T. (1988). A spiral nerve cuff electrode for peripheral nerve stimulation, *IEEE Transactions on Biomedical Engineering* **35**(11): 905–916.

NSCISC (2018). Spinal cord injury facts and figures at a glance, National Spinal Cord Injury Statistical Center.

Peckham, P. H., Keith, M. W., Kilgore, K. L., Grill, J. H., Wuolle, K. S., Thrope, G. B., Gorman, P., Hobby, J., Mulcahey, M., Carroll, S., Hentz, V. R. & Wiegner, A. (2001). Efficacy of an implanted neuroprosthesis for restoring hand grasp in tetraplegia: a multicenter study, *Archives of physical medicine and rehabilitation* **82**(10): 1380–1388.

Peckham, P., Mortimer, J. & Marsolais, E. (1976). Upper and lower motor neuron lesions in the upper extremity muscles of tetraplegics, *Spinal Cord* **14**(2): 115–121.

Pedrocchi, A., Ferrante, S., Ambrosini, E., Gandolla, M., Casellato, C., Schauer, T., Klauer, C., Pascual, J., Vidaurre, C., Gföhler, M. et al. (2013). MUNDUS project: MUltimodal Neuroprosthesis for daily Upper limb Support, *Journal of NeuroEngineering and Rehabilitation* **10**(1): 1–20.

Polasek, K. H., Hoyen, H. A., Keith, M. W., Kirsch, R. F. & Tyler, D. J. (2009). Stimulation stability and selectivity of chronically implanted multicontact nerve cuff electrods in the human upper extremity, *IEEE Transactions on Neural Systems and Rehabilitation Engineering* **17**(5): 428–437.

Rasmussen, C. E. & Williams, C. K. I. (2006). *Gaussian Processes for Machine Learning*, The MIT Press, Cambridge, MA.

Razavian, R. S., Ghannadi, B., Mehrabi, N., Charlet, M. & McPhee, J. (2018). Feedback control of functional electrical stimulation for 2-d arm reaching movements, *IEEE Transactions on Neural Systems and Rehabilitation Engineering* **26**(10): 2033–2043.

Rohm, M., Schneiders, M., Müller, C., Kreilinger, A., Kaiser, V., Müller-Putz, G. R. & Rupp, R. (2013). Hybrid brain–computer interfaces and hybrid neuroprostheses for restoration of upper limb functions in individuals with high-level spinal cord injury, *Artificial intelligence in medicine* **59**(2): 133–142.

Sartori, M., Reggiani, M., Farina, D. & Lloyd, D. G. (2012). Emg-driven forward-dynamic estimation of muscle force and joint moment about multiple degrees of freedom in the human lower extremity, *PloS one* **7**(12): e52618.

Schearer, E. M., Liao, Y., Perreault, E. J., Tresch, M. C., Memberg, W. D., Kirsch, R. F. & Lynch, K. M. (2014a). Indentifying inverse human arm dynamics using a robotic testbed, *International Conference on Intelligent Robots and Systems*, pp. 3585–3591.

Schearer, E. M., Liao, Y., Perreault, E. J., Tresch, M. C., Memberg, W. D., Kirsch, R. F. & Lynch, K. M. (2014b). Multi-muscle FES force control of the human arm for arbitrary goals, *IEEE Transactions on Neural Systems and Rehabilitation Engineering* **22**(3): 654–663.

Schearer, E. M., Liao, Y., Perreault, E. J., Tresch, M. C., Memberg, W. D., Kirsch, R. F. & Lynch,

K. M. (2015). Evaluation of a semiparametric model for high-dimensional FES control, *7th International IEEE EMBS Conference on Neural Engineering*, pp. 304–307.

Schearer, E. M., Liao, Y., Perreault, E. J., Tresch, M. C., Memberg, W. D., Kirsch, R. F. & Lynch, K. M. (2016). Semiparametric identification of human arm dynamics for flexible control of a functional electrical stimulation neuroprosthesis, *IEEE Transactions on Neural Systems and Rehabilitation Engineering* **24**(12): 1405–1415.

Schearer, E. M. & Wolf, D. N. (2019). Functional electrical stimulation capability maps, *2019 9th International IEEE/EMBS Conference on Neural Engineering (NER)*, IEEE, pp. 461–464.

Smith, B., Peckham, P. H., Keith, M. W. & Roscoe, D. D. (1987). An externally powered, multichannel, implantable stimulator for versatile control of paralyzed muscle, *IEEE Transactions on Biomedical Engineering* **34**(7): 499–508.

Smith, B., Tang, Z., Johnson, M. W., Pourmehdi, S., Gazdik, M. M., Buckett, J. R. & Peckham, P. H. (1998). An externally powered, multichannel, implantable stimulator-telemeter for control of paralyzed muscle, *IEEE Transactions on Biomedical Engineering* **45**(4): 463–475.

Valero-Cuevas, F. J. (2009). A mathematical approach to the mechanical capabilities of limbs and fingers, *Progress in motor control*, Springer, pp. 619–633.

Wolf, D. N. & Schearer, E. M. (2018). Holding static arm configurations with functional electrical stimulation: A case study, *IEEE Transactions on Neural Systems and Rehabilitation Engineering* **26**(10): 2044–2052.

Zhang, Q., Hayashibe, M. & Azevedo-Coste, C. (2013). Evoked electromyography-based closed-loop torque control in functional electrical stimulation, *IEEE Transactions on Biomedical Engineering* **60**(8): 2299–2307.